

Biaxialformer: Leveraging Channel Independence and Inter-Channel Correlations in EEG Signal Decoding for Predicting Neurological Outcomes

Naimahmed Nesaragi, Hemin Ali Qadir, Per Steiner Halvorsen, and Ilanko Balasingham, *Member, IEEE*

Abstract—Accurate decoding of EEG signals requires comprehensive modeling of both temporal dynamics within individual channels and spatial dependencies across channels. While Transformer-based models utilizing channel-independence (CI) strategies have demonstrated strong performance in various time series tasks, they often overlook the inter-channel correlations that are critical in multivariate EEG signals. This omission can lead to information degradation and reduced prediction accuracy, particularly in complex tasks such as neurological outcome prediction. To address these challenges, we propose *Biaxialformer*, characterized by a meticulously engineered two-stage attention-based framework. This model independently captures both sequence-specific (temporal) and channel-specific (spatial) EEG information, promoting synergy and mutual reinforcement across channels without sacrificing CI. By employing joint learning of positional encodings, *Biaxialformer* preserves both temporal and spatial relationships in EEG data, mitigating the inter-channel correlation forgetting problem common in traditional CI models. Additionally, a tokenization module with variable receptive fields balance the extraction of fine-grained, localized features and broader temporal dependencies. To enhance spatial feature extraction, we leverage bipolar EEG signals, which capture inter-hemispheric brain interactions, a critical but often overlooked aspect in EEG analysis. Our study broadens the use of Transformer-based models by addressing the challenge of predicting neurological outcomes in comatose patients. Using the multicenter I-CARE data from five hospitals, we validate the robustness and generalizability of *Biaxialformer* with an average AUC 0.7688, AUPRC 0.8643, and F_1 0.6518 in a cross-hospital scenario.

Impact Statement—Decisions about continued treatment for comatose patients hinge on uncertain predictions of brain recovery, leaving families and clinicians in a difficult position. This work delivers a reliable AI-based forecast of recovery chances by analyzing routine EEGs, consistently across multiple hospitals. This clarity can guide doctors toward personalized treatment plans, reduce the performance of invasive or costly procedures with little benefit, and give families timely, trustworthy information when weighing care options. By translating complex EEG signals into actionable insights, this approach promises to improve patient

care, ease emotional burdens on families, and foster smarter resource allocation in critical care.

Index Terms—Electroencephalogram, transformer, attention mechanism, channel-independence, predicting neurological outcome, EEG classification.

I. INTRODUCTION

ANNUALLY, over 6 million cardiac arrests (CAs) occur worldwide, with survival rates ranging from 1% to 10% [1]. After resuscitation from CA, the majority of patients are comatose and treated at intensive care units (ICUs) [2]. Assessment of neurological outcomes in comatose CA survivors due to post-anoxic coma remains a persistent challenge in clinical practice [3], [4]. Electroencephalography (EEG) is one of the most available tools and the popular modality used for assessing unconscious patients, owing to its non-invasive nature, ease of use, and high temporal resolution [5]. EEG is inherently multivariate, meaning it comprises multiple time series, each representing the electrical activity recorded from a different electrode placed on the scalp. These time series capture rich information about brain function encoded in both intra-channel features within an electrode (e.g., frequency variations, power in specific bands, burst suppression patterns) and inter-channel features (e.g., correlations or differences in activity between electrodes, phase coherence). The interplay between these features holds crucial insights into brain states and intentions. However, the relative importance of these features can vary. For instance, sleep stage classification might prioritize intra-channel signatures of EEG signals to particular frequency bands based on the targeted sleep stage [6]. Conversely, inter-channel EEG features are heavily relied in motor imagery classification for identifying differences in activity between channels at certain time points, such as event-related desynchronization/synchronization [7].

In the context of neurological outcome prediction after CA, the challenge is further compounded by the complexity of brain dynamics during coma [8]. Here, both temporal dynamics within channels and spatial relationships across channels are critical for assessing brain function. For eg., burst suppression patterns within a channel may indicate severe brain injury leading towards poor prognosis, while inter-channel coherence may reveal preserved network connectivity, which is predictive of good prognosis [9]–[12]. This intricate balance between intra- and inter-channel information makes the underlying task more challenging. Moreover, the variability across patients adds another layer of complexity. EEG patterns

This work was supported in part by the Health South East Authority in Norway, Helse Sør-Øst RHF (HSØ: New Realtime Decision Support during Blood Loss using Machine Learning on Vital Signs) under Grant No. 19/00264–202, and Prosjektnummer 2020079.

N.Nesaragi and H. A. Qadir are with the Intervention Centre, Oslo University Hospital, 0372 Oslo, Norway (e-mail: naimahmed.nesaragi@gmail.com and hemina.qadir@gmail.com).

P.S. Halvorsen is with Intervention Centre, Oslo University Hospital 0372, Oslo Norway, and also with Institute of Clinical Medicine, Faculty of Medicine, University of Oslo, Oslo, Norway (e-mail: p.s.halvorsen@medisin.uio.no).

I. Balasingham is with the Intervention Centre, Oslo University Hospital 0372, Oslo Norway, and also with the Department of Electronic Systems, Norwegian University of Science and Technology, 7491 Trondheim, Norway (e-mail: ilanko.balasingham@medisin.uio.no).

in comatose patients can vary widely depending on individual factors, including the underlying cause of CA, duration of hypoxia, comorbidities, and post-resuscitation care. This results in a wide range of intra- and inter-channel feature variability, making it difficult to generalize across patients. Though multi-channel EEG streams aid in reducing the subjectivity of prognostic evaluation to some extent, a diverse variation still exists among intra- and inter-channel features. So, selecting the most suitable feature information becomes crucial. Several prognostic features e.g., burst suppression, and nonreactive EEG patterns have already been identified based on the outcome of interest. However manual interpretable quantification of multivariate EEG streams is a laborious task that demands advanced clinical and neuro-physiological expertise, limiting the accessibility of EEG-informed prognostication. Hence, automating EEG interpretation can overcome these barriers, enhancing accessibility and diagnostic accuracy in clinical settings.

Deep learning (DL) techniques have recently been increasingly applied to multivariate time series (MTS) EEG data, offering a promising solution to the challenges of Brain-Computer Interface analysis. Based on modeling the variable dependencies, transformer-based models in general MTS can be broadly bifurcated into *channel-independence (CI)* and *channel-dependence (CD)*, also called channel-mixing models [13]–[16]. Although *CI* methods like PatchTST [17] that focus on intra-channel processing typically claim to yield better results, they overlook the potential complex interrelationships between different channels of MTS data. Conversely, *CD* methods like Crossformer [18], and iTransformer [19] could offer improvements by leveraging inter-channel correlations, but may lead to inadequate extraction of mutual information, and in some cases, potentially introduce noises [14]. Nonetheless, these studies argue that the integration of uncorrelated (cross-variable) information in the *CD* strategy could decrease the potential improvement in MTS model performance. Based on the considerations outlined above, it is quite evident that the Transformer-based models still has substantial promise in multivariate EEG analysis, particularly if advancements are made in extracting meaningful information from inter- and intra-channel data. To substantiate this claim, we introduce a bi-axes transformer-based network called *Biaxialformer* that effectively leverages cross-variable information across inter-channels (electrodes) while adequately extracting temporal information of intra-channel (time-steps) simultaneously. *Biaxialformer* introduces a sequence-channel-aligned two-stage attention structure that allows it to capture both temporal correlations among EEG sequences and dynamical dependence among multiple electrodes over time. To efficiently utilize a two-stage attention structure, we first design a joint learning of positional encodings to enhance the Transformer’s ability to model the spatiotemporal dynamics of EEG signals. The joint learning by positional encoding ensures that the model captures the spatiotemporal structure of the EEG data, which is crucial for tasks that require an understanding of both temporal patterns (e.g., rhythms, spikes) and spatial correlations (e.g., between neighboring electrodes). In this study, we hypothesize that a two-stage multi-head attention mechanism (MHA) can

enhance the predictive power of multichannel EEG data to classify comatose patients with good or poor neurological outcomes. Specifically, we propose that the fusion of intra- and inter-channel attention mechanisms can effectively discern attention patterns within individual EEG sequences and cross-attention patterns among multiple EEG channels. We summarize our key contributions as follows:

- We propose a two-stage MHA Transformer-based model that enhances both intra- and inter-channel features, promoting effective *CI* by independently modeling each channel’s temporal sequence simultaneously leveraging cross-variable information across electrodes.
- Our model incorporates joint learning of temporal and spatial positional encodings to address inter-channel correlation forgetting, a common issue in *CI* models.
- We design a token fusion module with adjustable receptive fields, optimizing the balance between localized features and broader temporal dependencies.

II. REALTED WORK

A. *CI* and *CD* modeling and Transformer-based models for EEG decoding

Many existing transformer-based time series prediction models have modeled global dependencies well. In the case of time series transformers, the longer the lookback window, the lower the performance, and the limitation is that computation increases explosively [19]. A vanilla transformer architecture embeds each time step across multivariate time-series as a temporal token leading to a mixed variate representation [19]. Unified embedding by each temporal token may fail to learn a variate-centric representation of multiple series or create a meaningless attention map. In other words, existing time series transformer-based models struggle to establish multivariate correlation.

PatchTST [17] architecture splits the time series data into patches, allowing it to maintain *CI* between different variables in the data. It divides lengthy time series into manageable *patches* enabling efficient processing and capturing fine-grained patterns. *CI* in PatchTST refers to the idea that instead of processing all channels together, it analyzes them individually, unlocking unique insights within each data stream. However, while this approach excels at isolating and focusing on intra-channel features, it can struggle with inter-channel dependencies, potentially missing important long-range interactions between different channels. In other words, *CI* offered by PatchTST is a double-edged sword. This channel isolation can limit the model’s ability to capture interactions between channels in MTS, leading to a phenomenon known as channel mixing.

Further, iTransformer [19] implementation tries to mitigate this problem of channel mixing where instead of several channels being embedded at once for each specific time-point, iTransformer embeds each univariate channel as an individual token. This leads to an advantage of variate-unmixed representation where each channel’s contribution is modeled independently, allowing the model to avoid interference between less relevant channels. However, this strategy reduces the overall number of tokens available for each channel, and while it

enables greater *CI*, it may limit the model's ability to capture long-range dependencies across channels due to its larger receptive field. iTransformer offers a compromise, enabling some *CI* through masking, while still allowing interaction modeling via inter-channel relationships.

This variation in feature importance results in the challenge of effectively capturing these diverse intra- and inter-channel features across various EEG coding tasks, so selecting the most suitable model architecture becomes crucial. In summary, Patch-based transformer architectures like PatchTST excel at capturing intra-channel features due to their strong *CI*, making it ideal for EEG tasks where individual channel processing is crucial, such as sleep stage classification. However, such architectures may struggle with capturing long-range inter-channel dependencies needed for tasks like motor imagery classification. Conversely, transformer architectures like iTransformer effectively model inter-channel interactions for tasks involving long-range dependencies but may face challenges in isolating the independent contributions of each channel due to the increased potential for interference across channels.

However, Transformer-based models in general have demonstrated improved predictive performance by refining the attention mechanism and have presented an intriguing avenue for further exploration of the multi-channel integration of the brain [20]. Few Transformer-based schemes [21]–[25] have garnered attention and brought into EEG decoding applications but are confined mostly to motor-imagery classification tasks such as emotion recognition, and classification of sleep stages and imagined speech. Most of these studies are limited to the usage of within-subject and within-session applications, limiting the transformer model's robustness for different individuals [26], [27]. Hence, there is a critical need to extend the evaluation of transformer-based networks on EEG decoding beyond these aforementioned applications.

B. Automated schemes for predicting neurological outcomes

The recent modest literature on predicting neurological outcomes using EEG recordings stems from the PhysioNet 2023 Challenge [5], [28] that aimed at the development of various automated schemes focused on enhancing true positive rate (TPR) for predicting a poor outcome given a false positive rate (FPR) ≤ 0.05 at 72 hours after the return of spontaneous circulation (ROSC). Most of these state-of-art submissions [28]–[30] rely on machine-learning (ML) methods using extraction of hand-crafted EEG features like statistical, power in frequency bands, entropy values, etc., from multiple domains or transfer learning using pre-trained models [31], as it is more challenging to extract the required EEG feature representation for the desired type of neurological outcome. Further, ML studies mostly predict outcomes based on EEG patterns observed within a specific time window, without utilizing the temporal evolution of the EEG data [32].

Contemporary research on the prediction of neurological outcomes in comatose patients has employed various DL techniques to gain insight into EEG data by sequence modeling, and has yielded satisfactory predictive performances [33]–[36]. However, with hindsight, providing a straightforward comparison among these studies is tedious since, the context

or focus of interest in the predicted outcome is different, and variability exists in the definitions of prediction windows [8]. Regardless of faithful results obtained by these DL models for the prediction of neurological outcomes, the existing literature is naïve towards the noteworthy application of the transformer-based model [37], [38] that can capture the spatiotemporal structure of the sparse MTS EEG data, crucial for tasks that require understanding both temporal patterns among EEG sequences and spatial correlations between neighboring electrodes.

III. MATERIALS

A. Study Population

The data considered under this study originates from the recent PhysioNet/Computing in Cardiology Challenge 2023 [5], [28]. This data is retrieved from ICU patients of seven academic hospitals in the U.S. and Europe led by investigators in the International Cardiac Arrest REsearch consortium (I-CARE). The goal is to employ EEG recordings to predict neurological outcomes among comatose patients after CA. Neurological function was determined using the Cerebral Performance Category (CPC) scale. CPC is an ordinal scale ranging from 1 to 5 with “Good outcome”: CPC = 1 or 2, “Poor outcome”: CPC = 3, 4, or 5.

This multi-center databases has adult patients with in-hospital or out-of-hospital CA who had ROSC but remained comatose. Each patient's brain activity was monitored with a 19-channel continuous EEG. Monitoring is typically started within hours of CA and continues for several hours to days depending on the patient's condition, so recording start time and duration varied from patient to patient. The databases includes EEG data obtained up to 72 hours from ROSC. Challenge organizers obtained the consent of approval from the appropriate institutional review boards to collect data [5], [28]. The data were split into training, validation, and test sets. The training set comprises of 607 patients (approximately 60%), while 10% of patients in the validation set, and 30% in the test set. The proposed study has used the publicly shared dataset of 607 patients from five hospital centers (A, B, D, E, F) for the experiments in leave-one-out center format. Detailed statistics are mentioned in Table I.

TABLE I
DISTRIBUTION OF NEUROLOGICAL OUTCOMES IN PUBLICALLY SHARED TRAINING COHORT

Hospital code	Good Outcomes	Poor Outcomes	Total	Study Dataset (%)	Poor Outcomes (%)
A	122	139	261	43.00	53.26
B	34	86	120	19.77	72.00
D	27	56	83	13.67	67.47
E	15	59	74	12.19	79.73
F	27	42	69	11.37	60.87
Total	225	382	607	-	-

B. Pre-Processing

The data pre-processing pipeline includes the following sequence of operations: filtering, re-sampling, rescaling, bipolar conversion, and finally, segmentation of EEG recordings. At the onset, the entire EEG data is filtered using a Butterworth

band pass filter with cut-off frequencies of 0.5 Hz and 35 Hz to remove baseline wander and high-frequency noises from the EEG signals. Next, the filtered signals are examined in terms of sampling frequency, and all the EEG recordings are re-sampled to 100 Hz to maintain uniformity w.r.t sampling frequencies. The re-sampled signals are then re-scaled using Min-max standardization. Next, re-scaled signals are converted to bipolar representations and finally segmented. The bipolar conversion, subtracting EEG signals from adjacent scalp electrodes, is crucial in EEG signal processing [39]. It reduces noise and artifacts, enhances spatial resolution by focusing on localized brain activity, minimizes volume conduction effects, and aids comparisons to baseline states. It is valuable in clinical and neuroscience research and provides a cleaner and more accurate brain activity representation [40]. This data pre-processing pipeline yields 18 bipolar channels from every hour of EEG recordings.

Further, in our study, we employ a systematic approach to process n -minute EEG segments into subseries-level patches by the tokenization module (see subsection IV-A). We adopt the idea of patching [17] since patches can better capture local information and also encompass richer dependencies between EEG channels and sequences.

Let \mathbf{X} denote a multivariate time-series EEG dataset with m samples of n -minute segments given as,

$$\mathbf{X} = \left\{ \mathbf{x}_1^{(t,k)}, \mathbf{x}_2^{(t,k)}, \dots, \mathbf{x}_m^{(t,k)} \right\} \quad (1)$$

where, $\mathbf{x}_i^{(t,k)} \in \mathbb{R}^{C \times L}$, $t = 0, 1, \dots, L$; $k = 0, 1, \dots, C$.

C denotes the number of EEG channels and L denotes the length in samples of each EEG sequence corresponding to n -minute multivariate EEG array segment. L in samples is computed as $L = n \times f_s \times 60$, where f_s is the sampling frequency.

Let $\mathbf{x}_i^{(k)} \in \mathbb{R}^C$ represent the values of the various channels at the t -th time point and let $\mathbf{x}_i^{(t)} \in \mathbb{R}^L$ denote the input univariate EEG time series of the k -th channel. Let \mathbf{Y} denote label set for the corresponding EEG dataset \mathbf{X} with m samples given as,

$$\mathbf{Y} = \left\{ \mathbf{y}_1, \mathbf{y}_2, \dots, \mathbf{y}_m \right\} \quad (2)$$

where, $\mathbf{y}_i \in \{0, 1\}$, 0- Good, 1- Poor.

IV. METHODS

As shown in Fig.1, the model consists of four main components: (i) *Tokenization Module* block encodes the high-frequency raw EEG signal information into token embeddings. (ii) *Intra-channel embedding* block encodes the compressed and auxiliary augmented EEG data (with positional encoding and intra-channel class tokens) along the temporal axis. Subsequently, the intra-channel class tokens containing the temporal features within each EEG channel are generated. (iii) *Inter-channel embedding* block encodes temporally segmented and auxiliary augmented EEG data (with positional encoding and inter-channel class tokens) along the channel axis. Subsequently, inter-channel class tokens capture significant information about the relationships between the channels within each

patch at a specified time. (iv) *Temporal-spatial fusion* block effectively fuses intra- and inter-channel information to extract significant features from the EEG data.

A. Tokenization Module

The input to the tokenization module is fed in terms of batches B given as,

$$\mathbf{X}_B = \left\{ \mathbf{x}_1^{(t,k)}, \mathbf{x}_2^{(t,k)}, \dots, \mathbf{x}_B^{(t,k)} \right\} \quad (3)$$

where each input batch $\mathbf{X}_B \subseteq \mathbf{X}$ with batch size $B \leq m$. The tokenization module then converts the signal patches into token embeddings by applying tokenization through a module architecture similar to the wav2vec [41]. Our proposed architecture of tokenization comprises an independent feature encoder (FE) per channel. Hence we have C feature encoders as shown in Fig. 2. Each FE block is a stack of l 1-D convolutional neural network (CNN) layers that excel at capturing local patterns and dependencies within the EEG channels w.r.t time, effectively reducing the data dimensionality while preserving relevant sequence-level semantic information. This feature extraction process transforms raw EEG signals into compact representations as tokens that the *intra- and inter-channel embedding blocks* can further process. Tokenization allows the EEG data to be organized into discrete fragments, enabling the attention mechanism to model long-range dependencies and capture complex relationships within inter- and intra-EEG channels. The initial layer of FE includes an *instance normalization* between the 1-D convolution and the *Gaussian Error Linear Unit* (GELU) activation function, while the other layers consist of a 1-D convolution followed by a GELU activation function.

The total context of the FE receptive field is a critical parameter in time-series analysis, as it determines the temporal context captured by each token in time-series modeling. In EEG signals, which are characterized by high temporal resolution and dynamic patterns, selecting an appropriate receptive field is essential to accurately capture relevant neural activity. A larger receptive field allows the model to capture long-range dependencies and broader contextual information, which is crucial for identifying patterns across extended periods. Conversely, a smaller receptive field focuses on fine-grained, localized patterns, which may be important for detecting transient or rapidly changing neural events. In this study, we design a varying receptive field by adjusting kernel sizes and strides to optimize the balance between capturing detailed, localized features and broader temporal dependencies, which is key to enhancing the model's ability to interpret and predict neural dynamics effectively. The total context of the FE receptive field (r) at the l^{th} layer is given by (4) [42]

$$r_i = r_{i-1} + (h - 1) \prod_{h=1}^{i-1} s_h \quad (4)$$

The first step to derive (4) is to calculate the number of tokens (output feature map) for each layer. This is calculated by (5):

$$o_i = \frac{o_{i-1} + 2p - h}{s} + 1 \quad (5)$$

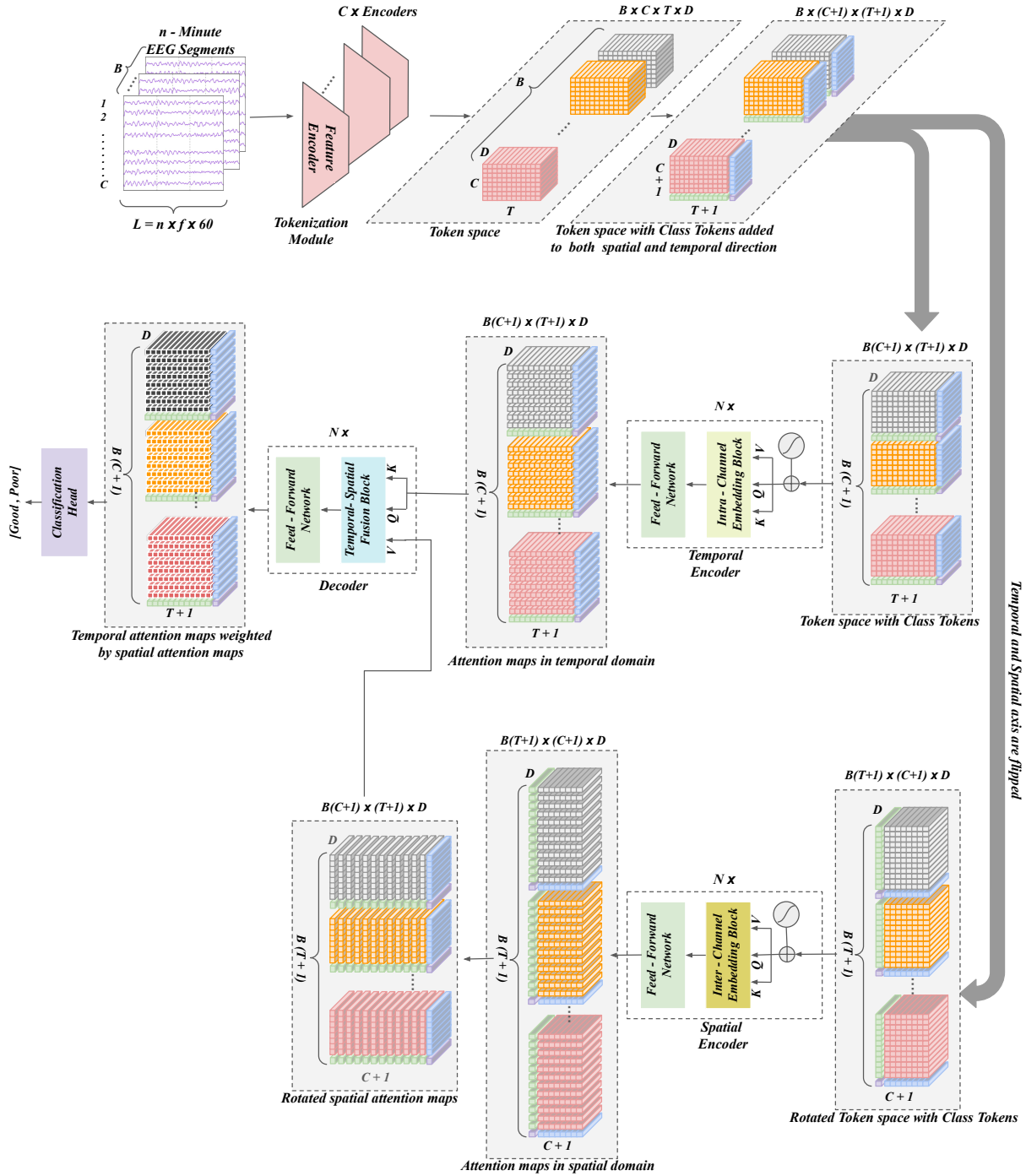


Fig. 1. *Biaxialformer* framework: A processed n -minute segment is fed to *Tokenization* block which converts each bipolar channel input to *Tokens* preserving local patterns and spatial relationships. The information about the position of each token in the sequential feature space is encoded twice by the joint *Positional Encoding*. The *Biaxialformer* focuses on relevant information between intra- and inter-channels by utilizing Temporal and Spatial encoders respectively. Outputs of the two encoders are then fused by the Decoder. Resulting attention maps are flattened and fed to the classification head for binary classification.

where o_i is the number of the output features for layer i , o_{i-1} is the number of the input features, p is the padding size, h is the kernel size and s is the stride of the layer i . Next, we need to calculate the jump (j) which in general, represents the cumulative stride. We can get j by multiplying the strides of all layers before the current layer under investigation as follows:

$$j_i = j_{i-1} * s \quad (6)$$

where j_{i-1} is the jump of the previous layer. Finally, using previous values, we can calculate the size of the receptive field, using this formula:

$$r_i = r_{i-1} + (h - 1)j_{i-1} \quad (7)$$

The equation (4) is the more general form of the formula (7) that is used for calculating the receptive field of l^{th} layer. It is to be noted that, each input univariate EEG series

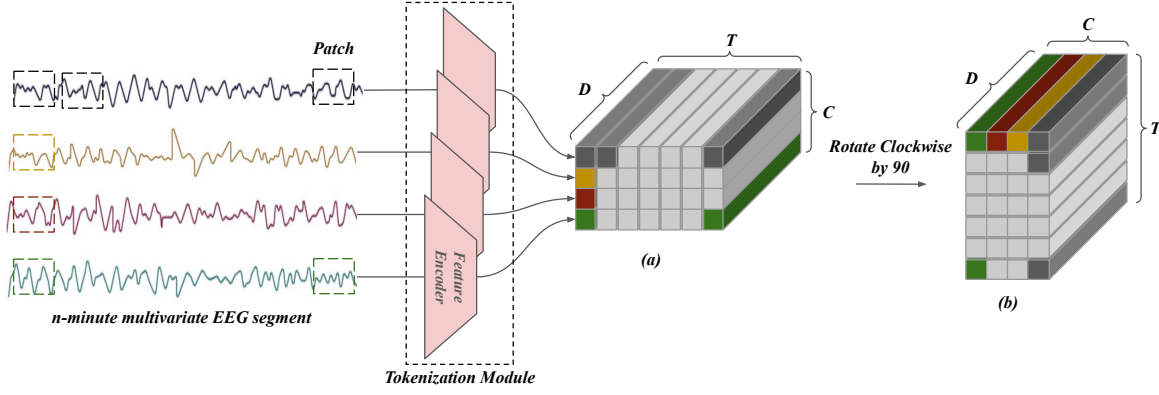


Fig. 2. Conversion of signal patches into token embeddings from a typical 4-channel EEG array as an example for two scenarios (a) intra-channel (temporal), and (b) inter-channel (spatial). Each EEG sequence (L) in a n -minute EEG segment is divided into patches. Based on stride (s) and with the corresponding reception field (r) of the feature encoder, each patch is converted into token embedding. In total T tokens each with model dimension (D) are generated from a n -minute EEG segment.

is converted into patches by the corresponding FE that can serve as input tokens to the attention mechanism. Given s as stride between two consecutive patches and D as token length (model dimension, 768), each FE unfolds the n -minute EEG array \mathbf{X}_B into the embedded tensor $\mathbf{Z}_B \in \mathbb{R}^{B \times C \times T \times D}$ where T is the number of patches, $T = \left\lfloor \frac{(L-D)}{s} \right\rfloor + 1$. For instance, the proposed tokenization module comprised seven embedding layers with the following kernel sizes of [10, 5, 5, 5, 5, 3, 3] and strides of [5, 3, 3, 3, 2, 3, 3] for r corresponding to ~ 30 seconds at the 100 Hz sample rate. Here values of r and j were 2970 and 2430 in samples respectively. Hence 12 tokens were generated from each channel in a 5-minute segment EEG array as shown in Fig. 3.

B. Positional encoding

The attention mechanism alone can not explicitly model the sequence token order (i.e., time steps or channels). Therefore, we employ a learnable additive positional encoding scheme to provide positional information about the tokens. Two separate positional encodings and class tokens in the intra- and inter-channel axes are added to encode temporal and spatial information respectively. The joint learning occurs as both sets of positional encodings (temporal and spatial) are learned together as part of the overall model's training process. The proposed joint learning of positional encodings addresses the challenge of *inter-channel correlation forgetting* [15] in MTS analysis, such as EEG signals, by ensuring that spatial dependencies between channels are explicitly modeled alongside temporal dynamics. Traditional MTS models often focus on temporal relationships within each sequence (or channel), leading to a neglect of spatial correlations between channels, especially when they are processed independently. This can result in channel correlation forgetting, where important inter-channel interactions, such as those critical in EEG data (e.g., neural oscillations or network activities spanning multiple electrodes), are lost. At the same time, this architecture promotes effective CI by ensuring that each channel's temporal sequence is modeled independently via intra-channel encoding, allowing the model to recognize unique patterns within each channel. Since EEG arrays are MTS representations, we assumed that information on the temporal order is significant for comprehending the relationship between channels. So, we first append $B \times C$ number of class tokens (intra-channel class tokens), $\text{CLS}_{\text{intra}} \in \mathbb{R}^{B \times C \times D}$, at the beginning of the temporal axis, followed by $B \times (T+1)$ number of class tokens (inter-channel class tokens), $\text{CLS}_{\text{inter}} \in \mathbb{R}^{B \times (T+1) \times D}$ along channel axis. Once both class tokens are appended, we then add intra-channel-wise learnable positional encoding, $\mathcal{W}_{\text{pos-intra}} \in \mathbb{R}^{B \times C \times (T+1) \times D}$, at the beginning of the temporal axis. This temporally divided data, with the dimension $B \times C \times (T+1) \times D$ is then subjected to inter-channel-wise learnable positional encoding $\mathcal{W}_{\text{pos-inter}} \in \mathbb{R}^{B \times (C+1) \times (T+1) \times D}$, along the channel axis. The overall shape of the resultant feature

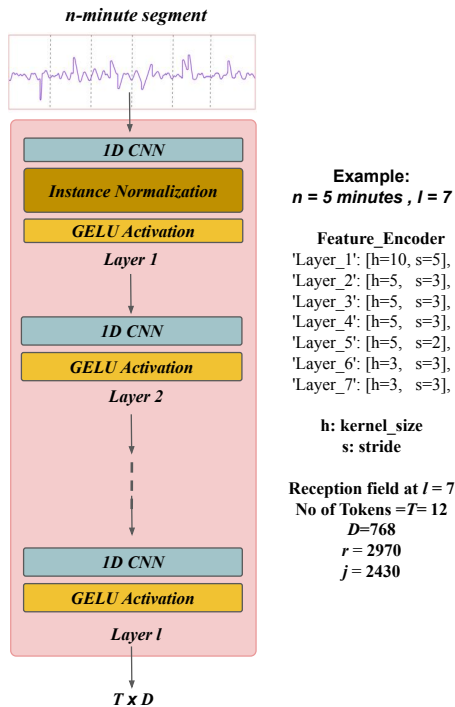


Fig. 3. Single FE design.

maps is $B \times (C + 1) \times (T + 1) \times D$. The positional encoding and class tokens are added simultaneously to ensure that, the data size remains consistent before and after processing. The resultant feature maps will be further subjected to two-stage multi-head attention (MHA) separately.

C. Intra Channel Embedding Block (Temporal)

This embedding block utilizes a native Transformer encoder design [43], [44] to model the EEG signals' temporal features. This block employs MHA and a feed-forward network on channel-wise-divided data to encode significant intra-channel information. To achieve this the channel and batch axis of the feature maps were merged resulting in dimension $B(C + 1) \times (T + 1) \times D$. This results in a reshaped representation where each EEG channel is treated independently with its corresponding temporal data for further processing. The MHA mechanism focuses on learning temporal dependencies within each channel to build patch-wise attention. For this, the data is projected into three distinct subspaces to compute attention scores using learnable matrices Q_T , K_T , and V_T , where each corresponds to the temporal patch tokens (time-steps). *Query* (Q_T): a projection of the input data that defines the information the model seeks in the temporal dimension. *Key* (K_T): a second projection that represents the potential locations where relevant information might be found, i.e., temporal positions in the sequence. *Value* (V_T): a third projection containing the actual content or features at each time step (patch) that are to be retrieved based on the query-key matching process. These matrices are learned during training and can be described as:

$$Q_T = Z_T \mathcal{W}_{Q_T}, K_T = Z_T \mathcal{W}_{K_T}, V_T = Z_T \mathcal{W}_{V_T} \quad (8)$$

where Z_T is the input temporal data and \mathcal{W}_{Q_T} , \mathcal{W}_{K_T} , \mathcal{W}_{V_T} are the learned weight matrices that project the input into the query, key, and value spaces, respectively.

By aggregating these dependencies into class tokens, the model efficiently encodes the temporal information within each channel, ready for further processing and integration with spatial features from other channels.

D. Inter Channel Embedding Block (Spatial)

This embedding block also utilizes a native Transformer encoder design to model the EEG signals' spatial features. This block focuses on capturing spatial relationships between EEG channels, i.e., inter-channel dependencies within the same temporal slice or patch. After the intra-channel (temporal) encoding is completed, the original feature maps are restructured by merging the temporal and batch axes, resulting in a transformation with dimensions $B(T + 1) \times (C + 1) \times D$. This transformation enables the model to treat each time step (or patch) across all channels as a single entity and apply attention to learn the inter-channel dependencies. Now, the inter-channel-wise MHA mechanism and a feed-forward network are employed on this resultant temporally divided data, to extract significant information between the EEG channels within a specific time. Similar to the intra-channel attention, three learnable matrices — Q_S , K_S , and V_S are used to construct attention scores, but this time across channels at a specific temporal slice, rather than across time steps within a channel. The learnable matrices are defined as: *Query* (Q_S):

represents the current EEG channel, indicating which inter-channel relationships to focus on within the current temporal slice. *Key* (K_S): represents the potential spatial relationships between channels, i.e., how one EEG channel's information can be related to others. *Value* (V_S): holds the actual content or features of each channel, which will be weighted based on how relevant each channel is to the others. The matrices are calculated as:

$$Q_S = Z_S \mathcal{W}_{Q_S}, K_S = Z_S \mathcal{W}_{K_S}, V_S = Z_S \mathcal{W}_{V_S} \quad (9)$$

where Z_S represents the transformed feature maps where each token corresponds to an EEG channel at a specific time step, and \mathcal{W}_{Q_S} , \mathcal{W}_{K_S} , \mathcal{W}_{V_S} are the learned weight matrices. After computing the inter-channel-wise attention, the model aggregates the spatial dependencies between EEG channels into inter-channel class tokens. Each class token represents a summary of the relationships between the channels for a specific temporal slice, encapsulating the spatial structure of the EEG data at that time.

Thus, by employing and operating two-stage attention mechanisms jointly, we could encode inter- and intra-channel information from the downsampled EEG patches. The two embedding blocks operate independently using two different types of class tokens. The reuse of feature maps derived from tokenization undergoes a reshape operation to seamlessly transition the two-stage MHA operations for inter- and intra-channel information respectively. By this, we achieve devoid of direct inter-informational exchange, potentially resulting in a lack of coordinated feature extraction across channels and sequences. This intricate design aims to establish a cohesive interplay between temporal and spatial representations, ensuring a harmonized extraction of EEG features.

E. Temporal-Spatial Fusion Block (Decoder)

This block is designed to integrate the outputs from the intra-channel (temporal) and inter-channel (spatial) encoders through a *Cross-attention* (CR) mechanism. This CR process leverages the information encoded separately by the temporal and spatial encoders to create a unified representation of the EEG data, combining both time and channel relationships. The model then effectively integrates temporal and spatial information through MHA, producing a fused representation that captures the critical relationships between EEG channels and their temporal evolution. The decoder's CR operates by mapping the Values from the spatial encoder and the Query-Key pairs from the temporal encoder to compute the final fused output. The attention mechanism is built using three learnable matrices: *Query* (Q_{ST}): extracted from the temporal encoder's output, representing the temporal features (intra-channel information). *Key* (K_{ST}): also derived from the temporal encoder, providing the reference points that determine which temporal features are relevant to the spatial information. *Value* (V_{ST}): taken from the spatial encoder's output, representing the inter-channel (spatial) information to be retrieved based on the temporal query-key matching. These matrices are defined as:

$$Q_{ST} = Z_{to} \mathcal{W}_{Q_{ST}}, K_{ST} = Z_{to} \mathcal{W}_{K_{ST}}, V_{ST} = Z_{so} \mathcal{W}_{V_{ST}} \quad (10)$$

where Z_{to} is the output feature maps from the FE and, Z_{so} is output from the spatial encoder. $\mathcal{W}_{Q_{ST}}, \mathcal{W}_{K_{ST}}, \mathcal{W}_{V_{ST}}$ are the learned weight matrices.

The final output is computed as a weighted sum of the values, where the weight assigned to each value is computed by a compatibility function of the query with the corresponding key. The compatibility function computes attention scores by taking the dot product of the Query (from the temporal encoder) and Key (also from the temporal encoder), as follows:

$$CR(Q_{ST}, K_{ST}, V_{ST}) = \text{Softmax} \left(\frac{Q_{ST}(K_{ST})^T}{\sqrt{d_k}} \right) V_{ST} \quad (11)$$

Here, $\sqrt{d_k}$ is the dimension of the Key, ensuring the dot product is scaled appropriately for numerical stability. The attention scores represent how well each temporal Query aligns with the Keys, determining which temporal features are relevant to the spatial features encoded in the Value matrix. Once the attention scores are calculated, they are applied to the Value matrix (from the spatial encoder) to compute a weighted sum. This weighting allows the model to focus on the spatial features that are most relevant to the temporal features, effectively fusing the temporal and spatial information.

F. Classification head

The classification head converts high-dimensional decoder representations into a final prognosis of either 'poor' or 'good.' It receives weighted attention maps that capture temporal and spatial relationships within the EEG data. These maps are flattened into a one-dimensional vector of size $(C+1) \times (T+1) \times D$, then passed through a fully connected layer. A softmax layer applied to the logits produces probabilities reflecting the model's confidence in each prognosis category.

V. EXPERIMENTAL SETUP

A. Scoring Metric

The scoring metric (SM) is TPR for predicting a poor outcome (CPC of 3, 4, or 5) given an FPR ≤ 0.05 at 72 hours after the ROSC.

$$SM = \frac{TP}{TP + FN} \Big|_{FPR \leq 0.05}, 72h \text{ after ROSC} \quad (12)$$

The clinical rationale for evaluating the algorithm's performance using the TPR at a FPR of 0.05 is as follows. In clinical settings, prognostic assessments play a crucial role in deciding whether to continue life-supporting interventions. A false-positive prediction of poor outcome is particularly concerning, as it may lead to the withdrawal of life support from a patient who has the potential to recover consciousness, resulting in their death. While false negatives—failing to predict a poor outcome, thereby prolonging life support in patients who ultimately have a poor prognosis—are also challenging, they are generally considered less critical than false positives. Consequently, professional society guidelines recommend that prognostic tests maintain a FPR of 5% or lower.

There are two key reasons for assessing the algorithm's performance at 72 hours, rather than at earlier time points. First, research suggests that EEG trends over time provide valuable

prognostic information [32]. Second, premature predictions of poor neurologic outcomes may lead to self-fulfilling prophecies. Therefore, it is recommended to delay formal neurologic prognoses until at least 72 hours post-event.

B. Implementation details & Evaluation Settings

Adam optimizer is applied to update the model's weights with a batch size of 10 and a learning rate 0.0001 for 40,000 iterations. A cosine annealing schedule is employed to decay the learning rate during training. For the binary classification task of the neuro-prognostication, we utilized the binary cross-entropy loss function to guide the training, tailored to the 'Good' and 'Poor' neurological outcome labels:

$$L_{(\hat{y}, y)} = -\frac{1}{N} \sum_{i=1}^N [y_i \log(\hat{y}_i) + (1 - y_i) \log(1 - \hat{y}_i)] \quad (13)$$

where N is the batch size, y_i is the true label ($y_i = 1$ for 'Good' and $y_i = 0$ for 'Poor'), and \hat{y}_i is the predicted outcome for the i -th patient.

The inherent attention mechanism of the Transformer-based implementation typically requires a significant amount of training data to capture intrinsic correlations among EEGs. This is achieved by deploying a segmentation approach for the selected hour of EEG recording into 5-minute segments. To further robust the training process, each iteration is started by randomly selecting an hour of EEG recording of a patient, followed by a segmentation strategy, and then selecting a random 5-minute segment from the corresponding chosen random hour. Using this random selection and 5-minute segmentation techniques, we could generate ~ 0.5 million training samples from EEG recordings of 607 patients.

VI. RESULTS & DISCUSSION

A. Classification Results

The proposed study used the publicly shared training dataset of 607 patients from five hospital centers (A, B, D, E, F) for the experiments in a leave-one-out center format. Notably, hospital A accounts for half of the patients in the dataset. Since the original test dataset was not publicly made available after the challenge period, this study initiated a comprehensive experimental regimen, with the formulation of test-train splits. A cross-validation was performed individually on each of the five hospitals within the public training dataset. Consequently, each iteration of the in-house test set comprised solely one hospital, which had been held out from the training set. Subsequently, we compiled and reported the cross-validation results obtained for all participating hospitals across different time windows (in hours 12, 24, 48, 72), including the average results of various other performance metrics in Tables II, III. It is to be noted that throughout our study we chose the EEG segment duration to be 5 minutes, with $r = 30$ seconds. As shown in Table II, the SM is higher for the time window of 48 hours across all hospitals. This is attributed to the negatively skewed data distribution in the study (refer Fig.2 of [5]). Specifically, most patients across the five hospitals have data recorded for at least a day but less than three days. Further, Tables II, III show that hospitals D, E, and F performed well and consistently produced the expected results. However,

TABLE II
ASSESSMENT OF BIAXIALFORMER USING SM (TPR AT FPR OF 0.05) IN
LEAVE-ONE-CENTER-OUT FORMAT FOR DIFFERENT TIME-WINDOWS

Hospital	SM 12h	SM 24h	SM 48h	SM 72h
A	0.1742	0.3810	0.5120	0.4820
B	0.1650	0.2466	0.3270	0.2440
D	0.1856	0.3962	0.5792	0.5144
E	0.1860	0.3662	0.8204	0.7798
F	0.1200	0.4846	0.5802	0.5619

hospital A had a slightly lower SM of 0.4820. Since hospital A represents about 43% of the study population, the model was consequently trained on slightly fewer patients compared to the other four hospitals, which likely contributed to its reduced performance in this case. While Hospital B's SM may seem low, its other performance metrics still reveal good predictive performance. The lower custom SM, focused on a high TPR at an $FPR \leq 5\%$, emphasizes minimizing false alarms, and doesn't fully reflect the model's ability to capture positive cases effectively. Given the possibility of unique patient characteristics in Hospital B's data, these alternative metrics underscore its reliability despite the stricter scoring criterion.

TABLE III
ASSESSMENT OF BIAXIALFORMER USING OTHER PERFORMANCE
METRICS IN LEAVE-ONE-CENTER-OUT FORMAT

Hospital	SM 72h	F1	AUROC	AUPRC
A	0.4820	0.6590	0.7980	0.8930
B	0.2440	0.5200	0.6210	0.7930
D	0.5144	0.6877	0.8210	0.9010
E	0.7798	0.7660	0.8490	0.9440
F	0.5619	0.6912	0.7619	0.8012
Avg.	0.5164	0.6518	0.7688	0.8643

B. Ablations

To demonstrate and validate the performance of Bi axialformer, we conducted targeted ablation studies, maintaining consistent model hyperparameters across all experiments. Hospital E was selected for these ablations and baseline comparisons, as it yielded the most favorable results in our cross-validation setup.

1) *Two-stage MHA architecture*: To verify the performance of the proposed two-stage MHA architecture in *Biaxialformer*, we conducted ablation studies that analyzed the individual contributions of the temporal and spatial encoder blocks. These experiments involved removing components of the two-stage MHA and evaluating their performance separately. Specifically, we trained two separate transformer encoder

TABLE IV
INTRA-CHANNEL (TEMPORAL) BLOCK RESULTS ON HOSPITAL E

Window	SM	F1	AUROC	AUPRC
12h	0.1642	0.4810	0.7120	0.7820
24h	0.3165	0.5466	0.8070	0.8440
48h	0.6856	0.6962	0.8792	0.9144
72h	0.5860	0.7162	0.8433	0.8710

models: one using only the intra-channel embedding block (temporal encoder) and the other using only the inter-channel embedding block (spatial encoder). In the first ablation, the *Biaxialformer* was trained using only the intra-channel block,

TABLE V
INTER-CHANNEL (SPATIAL) BLOCK RESULTS ON HOSPITAL E

Window	SM	F1	AUROC	AUPRC
12h	0.0932	0.4760	0.5937	0.6120
24h	0.2995	0.5376	0.7470	0.7961
48h	0.5849	0.6892	0.8672	0.8944
72h	0.4761	0.5962	0.8173	0.8413

excluding the inter-channel encoder. In the second setup, only the inter-channel block was considered. The results of these studies, as shown in Tables IV and V for Hospital E, demonstrate the individual contributions of temporal and spatial features, respectively. The results indicated that the full two-stage MHA architecture, with the temporal-spatial fusion block, significantly outperformed both individual ablations. Furthermore, the intra-channel embedding block outperformed the inter-channel embedding block, highlighting the difference in the amount of tokenization between them. In the intra-channel embedding block, the model tokenizes each time series (channel) into smaller temporal segments, and this fine-grained tokenization results in a larger number of tokens per channel, allowing the model to capture more detailed temporal patterns, including short-term dependencies like burst suppression, oscillatory patterns, and transient events.

The inter-channel embedding block, in contrast, focuses on modeling spatial relationships between different EEG channels. Here, the tokenization is typically coarser because the number of EEG channels is far fewer as compared to the length of time series data within each channel. While spatial dependencies in EEG (e.g., coherence between electrodes) are important, they don't require as many tokens because spatial interactions tend to evolve more slowly and are often more stable than temporal dynamics. Therefore, the inter-channel tokenization yields fewer tokens than the intra-channel block, limiting its overall contribution to the model's performance.

2) *Conditioning of Decoder*: In the original *Biaxialformer* architecture, the *Value* (V_{ST}) of the decoder is conditioned using Z_{so} . In this ablation, we condition the decoder on Z_{to} instead. Specifically, the cross-attention in Eq. (11) for the decoder is altered by replacing the V_{ST} input with Z_{to} , ensuring that the weighting of the attention maps for the final result is now focused on the temporal dimension. Table VI

TABLE VI
WEIGHTING FROM TEMPORAL AND SPATIAL ENCODERS ON HOSPITAL E

Conditioning	SM (72h)	F1	AUROC	AUPRC
Spatial weighted by Temporal	0.5762	0.6994	0.7972	0.8746
Temporal weighted by Spatial	0.7798	0.7660	0.8490	0.9440

furnish comparative results of this ablation versus original *Biaxialformer*. Our findings indicate that conditioning the decoder on Z_{so} yielded better results than Z_{to} . This can be attributed to the importance of spatial encoding in EEG data, where interactions between different brain regions (captured by spatial encoding) are crucial for tasks like neurological outcome prediction. Focusing on spatial features, the model can effectively capture inter-channel dependencies, leading to improved attention weighting and better performance. In

contrast, relying solely on temporal features may overlook these critical spatial dynamics, reducing prediction accuracy.

3) *Segment Variability & Window Size*: We conducted ablation studies exploring both window size and segment variability to assess the impact of segment selection and its duration on model performance. Initially, we tested the effect of varying the choice of window size from a given hour to 3, 10, and 12 minutes, instead of the 5 minutes used throughout the study. Table VII shows the optimal 5-minute window in the Biaxialformer architecture likely balances capturing temporal context and computational efficiency. While longer lookback windows, such as 10 or 12 minutes, can identify broader dependencies, they may dilute critical short-term features, increase computational costs, and risk overfitting or noise. Conversely, a 3-minute window may miss critical context, limiting feature extraction. We expanded this analysis by testing the effect of using multiple 5-minute segments from various hours per patient and aggregating predictions using a *mode* operation, revealing how varying the number of hours influences the SM for Hospital E. Table VII show that increas-

TABLE VII
SEGMENT VARIABILITY & WINDOW SIZE ON HOSPITAL E

Window Size (in mins)	-	3	5	10	12
SM (72h)	-	0.7152	0.7798	0.2319	0.1990
No.Segments (5 min)	1	5	7	9	11
SM (72h)	0.7798	0.8131	0.8255	0.8119	0.8012

ing the segment count improves the SM by capturing more representative temporal patterns. However, beyond a certain point, SM tapers off, indicating an optimal balance between EEG variability and computational efficiency, highlighting that strategic segment selection enhances robustness without redundancy.

TABLE VIII
EXPLORATION OF RECEPTION FIELD ON HOSPITAL E

Duration of r (secs)	30 secs	20 secs	15 secs	10 secs	5 secs
	$r=2970$ $j=2430$ $o=12$	$r=2160$ $j=2750$ $o=13$	$r=1620$ $j=2070$ $o=18$	$r=1080$ $j=1190$ $o=27$	$r=480$ $j=1050$ $o=61$
Tokenization Module (h, s)	10,5	10,5	10,5	10,5	10,5
	5,3	5,4	5,3	5,2	5,3
	5,3	5,3	5,3	5,2	5,2
	5,3	5,2	5,2	5,2	5,2
	5,2	5,2	5,2	3,3	3,2
	3,3	3,3	3,3	3,3	3,2
SM 72h	0.7798	0.7912	0.8471	0.7664	0.6823

4) *Exploration of reception field (r)*: We systematically explored the receptive field r of FE by varying kernel sizes and strides, resulting in different tokenization schemes. Each scheme produced distinct tokens, with r defined in terms of sample durations (seconds) for EEG signals. This ablation experiment aimed to identify the optimal r value that maximizes model performance by balancing the granularity of tokenization with the temporal context captured in each token.

Table VIII highlights classification results from Hospital E, with five different r values tested using a fixed window size of 5 minutes. Notably, an optimal value of $r = 15$ seconds, corresponding to 1500 samples ($f_s = 100Hz$), produced the best results, striking a balance between detail and broader context. With smaller r values (5 or 10 seconds), token counts increased (61 and 27 tokens, respectively), potentially leading to over-segmentation and loss of contextual information, despite retaining high granularity. Conversely, larger r values (20 or 30 seconds) reduced the token count to 13 and 12 tokens, which improved efficiency but led to a slight decline in performance, likely due to insufficient capture of finer temporal details.

C. Baselines

We demonstrate the performance of *Biaxialformer* by comparing it with the following baseline methods: 1) Three *CI* and *CD* Transformer-based modeling [17]–[19]; 2) Two Transformer-based models for EEG decoding [21], [25]. This

TABLE IX
RESULTS OF BASELINE-STUDIES ON HOSPITAL E

Method	SM	F1	AUROC	AUPRC
PatchTST [17]	0.2363	0.5365	0.6210	0.7730
iTransformer [19]	0.2935	0.5621	0.7210	0.7874
CrossFormer [18]	0.5460	0.6784	0.7878	0.8147
EEG-Conformer [21]	0.4456	0.6372	0.7145	0.7489
DFformer [25]	0.6142	0.7154	0.8383	0.8876
Biaxialformer	0.7798	0.7660	0.8490	0.9440

curated and comprehensive selection in Table IX aims to capture the diverse landscape of contemporary *CI* and *CD* Transformer modeling for MTS analysis in general and multi-channel EEG analysis. *Biaxialformer's* two-stage attention mechanism outperformed baseline models such as PatchTST, iTransformer, and Crossformer across multiple evaluation metrics, demonstrating its strength in modeling both intra- and inter-channel EEG features. PatchTST's *CI*, while effective for intra-channel analysis, led to a failure in capturing inter-channel correlations, resulting in lower prediction accuracy. iTransformer and Crossformer, while leveraging inter-channel dependencies, struggled to capture localized temporal patterns as effectively as *Biaxialformer*. The token fusion module in *Biaxialformer*, with its adaptive receptive fields, provided an ideal balance between short-term detail and long-range temporal dependencies, allowing for superior generalization across tasks. It is to be noted that DFformer shares conceptual similarities with our proposed *Biaxialformer*. However, DFformer still suffers from channel mixing, as in the second stage (inter-channel block) of MHA is sequentially fed with the previous, first stage MHA. *Limitations*: While *Biaxialformer* consistently outperformed the baselines, it is not without limitations. The trade-off between capturing localized and global features remains challenging, and future iterations could explore more dynamic tokenization techniques. Additionally, while iTransformer and Crossformer focus heavily on long-range dependencies, future work may further investigate how these aspects can be integrated more effectively with our framework to enhance long-term temporal modeling.

VII. CONCLUSION

In this study, we introduced *Biaxialformer*, a two-stage MHA Transformer-based model designed to address both intra-channel and inter-channel feature extraction in EEG signals. *Biaxialformer* effectively mitigates inter-channel forgetting, a common issue in traditional CI strategies, while avoiding the channel mixing seen in models that focus too heavily on inter-channel correlations. *Biaxialformer* demonstrated superior performance over baseline models such as PatchTST, iTransformer, and Crossformer, particularly in predicting neurological outcomes in comatose patients. The success of the temporal-spatial fusion block, particularly when conditioned on spatial dependencies, underscores the importance of balancing both local and global relationships within EEG data.

REFERENCES

- [1] R. Graham et al. Strategies to improve ca survival: a time to act. 2015.
- [2] M. Rundgren et al. Continuous amplitude-integrated electroencephalogram predicts outcome in hypothermia-treated cardiac arrest patients. *Critical care medicine*, 38(9):1838–1844, 2010.
- [3] A. O. Rossetti et al. Neurological prognostication of outcome in patients in coma after cardiac arrest. *The Lancet Neurology*, 15(6):597–609, 2016.
- [4] G. D. Perkins et al. Brain injury after cardiac arrest. *The Lancet*, 398(10307):1269–1278, 2021.
- [5] Edilberto Amorim, Wei-Long Zheng, Mohammad M Ghassemi, Mahsa Aghaeiaval, Pravinkumar Kandhare, Vishnu Karukonda, Jong Woo Lee, Susan T Herman, Adithya Sivaraju, Nicolas Gaspard, et al. The international cardiac arrest research consortium electroencephalography database. *Critical Care Medicine*, 51(12):1802–1811, 2023.
- [6] Reza Boostani, Foroozan Karimzadeh, and Mohammad Nami. A comparative review on sleep stage classification methods in patients and healthy individuals. *Computer methods and programs in biomedicine*, 140:77–91, 2017.
- [7] Chang S Nam, Yongwoong Jeon, Young-Joo Kim, Insuk Lee, and Kyungkyu Park. Movement imagery-related lateralization of event-related (de) synchronization (erd/ers): motor-imagery duration effects. *Clinical Neurophysiology*, 122(3):567–577, 2011.
- [8] Wei-Long Zheng, Edilberto Amorim, Jin Jing, Ona Wu, Mohammad Ghassemi, Jong Woo Lee, Adithya Sivaraju, Trudy Pang, Susan T Herman, Nicolas Gaspard, et al. Predicting neurological outcome from electroencephalogram dynamics in comatose patients after cardiac arrest with deep learning. *IEEE transactions on biomedical engineering*, 69(5):1813–1825, 2021.
- [9] C. Sandroni et al. Prediction of good neurological outcome in comatose survivors of ca: a systematic review. *Intensive care medicine*, 48(4):389–413, 2022.
- [10] A. O. Rossetti et al. Eeg predicts poor and good outcomes after cardiac ca: a two-center study. *Critical care medicine*, 45(7):e674–e682, 2017.
- [11] F. Bongiovanni et al. Standardized eeg analysis to reduce the uncertainty of outcome prognostication after ca. *Intensive Care Medicine*, 46:963–972, 2020.
- [12] B. J. Ruijter et al. Early eeg for outcome prediction of postanoxic coma: a prospective cohort study. *Annals of neurology*, 86(2):203–214, 2019.
- [13] Lu Han, Han-Jia Ye, and De-Chuan Zhan. The capacity and robustness trade-off: Revisiting the channel independent strategy for multivariate time series forecasting. *IEEE Transactions on Knowledge and Data Engineering*, 2024.
- [14] Haoxin Wang, Yipeng Mo, Nan Yin, Honghe Dai, Bixiong Li, Songhai Fan, and Site Mo. Dance of channel and sequence: An efficient attention-based approach for multivariate time series forecasting. *arXiv preprint arXiv:2312.06220*, 2023.
- [15] Wenyong Han, Tao Zhu, Liming Chen, Huansheng Ning, Yang Luo, and Yaping Wan. Mcformer: Multivariate time series forecasting with mixed-channels transformer. *IEEE Internet of Things Journal*, 2024.
- [16] Xue Wang, Tian Zhou, Qingsong Wen, Jinyang Gao, Bolin Ding, and Rong Jin. Card: Channel aligned robust blend transformer for time series forecasting. In *The Twelfth International Conference on Learning Representations*, 2024.
- [17] Yuqi Nie, Nam H Nguyen, Phanwadee Sinthong, and Jayant Kalagnanam. A time series is worth 64 words: Long-term forecasting with transformers. *arXiv preprint arXiv:2211.14730*, 2022.
- [18] Yunhao Zhang and Junchi Yan. Crossformer: Transformer utilizing cross-dimension dependency for multivariate time series forecasting. In *The eleventh international conference on learning representations*, 2023.
- [19] Yong Liu, Tengge Hu, Haoran Zhang, Haixu Wu, Shiyu Wang, Lintao Ma, and Mingsheng Long. itransformer: Inverted transformers are effective for time series forecasting. *arXiv preprint arXiv:2310.06625*, 2023.
- [20] Qianqian Shi, Junsong Fan, Zuoren Wang, and Zhaoxiang Zhang. Multimodal channel-wise attention transformer inspired by multisensory integration mechanisms of the brain. *Pattern Recognition*, 130:108837, 2022.
- [21] Yonghao Song, Qingqing Zheng, Bingchuan Liu, and Xiaorong Gao. Eeg conformer: Convolutional transformer for eeg decoding and visualization. *IEEE Transactions on Neural Systems and Rehabilitation Engineering*, 31:710–719, 2022.
- [22] Young-Eun Lee and Seo-Hyun Lee. Eeg-transformer: Self-attention from transformer architecture for decoding eeg of imagined speech. In *2022 10th International winter conference on brain-computer interface (BCI)*, pages 1–4. IEEE, 2022.
- [23] Zhe Wang, Yongxiong Wang, Chuanfei Hu, Zhong Yin, and Yu Song. Transformers for eeg-based emotion recognition: A hierarchical spatial information learning model. *IEEE Sensors Journal*, 22(5):4359–4368, 2022.
- [24] Dongyoung Kim, Jeonggun Lee, Yunhee Woo, Jaemin Jeong, Chulho Kim, and Dong-Kyu Kim. Deep learning application to clinical decision support system in sleep stage classification. *Journal of Personalized Medicine*, 12(2):136, 2022.
- [25] Sung-Jin Kim, Dae-Hyeok Lee, Heon-Gyu Kwak, and Seong-Whan Lee. Towards domain-free transformer for generalized eeg pre-training. *IEEE Transactions on Neural Systems and Rehabilitation Engineering*, 2024.
- [26] Jin Xie, Jie Zhang, Jiayao Sun, Zheng Ma, Liuni Qin, Guanglin Li, Huihui Zhou, and Yang Zhan. A transformer-based approach combining deep learning network and spatial-temporal information for raw eeg classification. *IEEE Transactions on Neural Systems and Rehabilitation Engineering*, 30:2126–2136, 2022.
- [27] Wenqie Huang, Wenwen Chang, Guanghui Yan, Zhifei Yang, Hao Luo, and Huayan Pei. Eeg-based motor imagery classification using convolutional neural networks with local reparameterization trick. *Expert Systems with Applications*, 187:115968, 2022.
- [28] Matthew A Reyna, Edilberto Amorim, Reza Sameni, James Weigle, Andoni Elola, Ali Bahrami Rad, Salmar Seyedi, Hyeokhyen Kwon, Wei-Long Zheng, Mohammad M Ghassemi, et al. Predicting neurological recovery from coma after cardiac arrest: The george b. moody physionet challenge 2023. In *2023 Computing in Cardiology (CinC)*, volume 50, pages 1–4. IEEE, 2023.
- [29] Morteza Zabihi, Alireza Chaman Zar, Pulkit Grover, and Eric S Rosenthal. Hyperensemble learning from multimodal biosignals to robustly predict functional outcome after cardiac arrest. In *2023 Computing in Cardiology (CinC)*, volume 50, pages 1–4. IEEE, 2023.
- [30] Hongliu Yang and Ronald Tetzlaff. Model ensembling for predicting neurological recovery after cardiac arrest: Top-down or bottom-up? In *2023 Computing in Cardiology (CinC)*, volume 50, pages 1–4. IEEE, 2023.
- [31] Dong-Kyu Kim, Hong-Cheol Yoon, Hyun-Seok Kim, Woo-Young Seo, and Sung-Hoon Kim. Predicting neurological outcome after cardiac arrest using a pretrained model with electroencephalography augmentation. In *2023 Computing in Cardiology (CinC)*, volume 50, pages 1–4. IEEE, 2023.
- [32] Wei-Long Zheng, Edilberto Amorim, Jin Jing, Wendong Ge, Shenda Hong, Ona Wu, Mohammad Ghassemi, Jong Woo Lee, Adithya Sivaraju, Trudy Pang, et al. Predicting neurological outcome in comatose patients after cardiac arrest with multiscale deep neural networks. *Resuscitation*, 169:86–94, 2021.
- [33] Marleen C Tjepkema-Cloostermans, Catarina da Silva Lourenço, Barry J Ruijter, Selma C Tromp, Gea Drost, Francois HM Kornips, Albertus Beishuizen, Frank H Bosch, Jeannette Hofmeijer, and Michel JAM van Putten. Outcome prediction in postanoxic coma with deep learning. *Critical care medicine*, 47(10):1424–1432, 2019.
- [34] Stefan Jonas, Andrea O Rossetti, Mauro Oddo, Simon Jenni, Paolo Favaro, and Frederic Zuber. Eeg-based outcome prediction after cardiac arrest with convolutional neural networks: Performance and visualization of discriminative features. *Human brain mapping*, 40(16):4606–4617, 2019.

- [35] Stanley DT Pham, Hanneke M Keijzer, Barry J Ruijter, Antje A Seeber, Erik Scholten, Gea Drost, Walter M van den Bergh, Francois HM Kornips, Norbert A Foudraine, Albertus Beishuizen, et al. Outcome prediction of postanoxic coma: A comparison of automated electroencephalography analysis methods. *Neurocritical care*, 37(Suppl 2):248–258, 2022.
- [36] Frederic Zubler and Athina Tzovara. Deep learning for eeg-based prognostication after cardiac arrest: from current research to future clinical applications. *Frontiers in neurology*, 14:1183810, 2023.
- [37] Chao-Chen Chen, Shavonne L Massey, Matthew P Kirschen, Ian Yuan, Asif Padiyath, Allan F Simpao, and Fuchiang Rich Tsui. Electroencephalogram-based machine learning models to predict neurologic outcome after cardiac arrest: A systematic review. *Resuscitation*, page 110049, 2023.
- [38] Hritvik Jain, Mohammed Dheyaa Marsool Marsool, Ramez M Odat, Hamid Noori, Jyoti Jain, Zaid Shakhatreh, Nandan Patel, Aman Goyal, Shrey Gole, and Siddhant Passey. Emergence of artificial intelligence and machine learning models in sudden cardiac arrest: A comprehensive review of predictive performance and clinical decision support. *Cardiology in Review*, pages 10–1097, 2024.
- [39] Dezhong Yao, Yun Qin, Shiang Hu, Li Dong, Maria L Bringas Vega, and Pedro A Valdés Sosa. Which reference should we use for eeg and erp practice? *Brain topography*, 32:530–549, 2019.
- [40] Hitten P Zaveri, Robert B Duckrow, and Susan S Spencer. On the use of bipolar montages for time-series analysis of intracranial electroencephalograms. *Clinical neurophysiology*, 117(9):2102–2108, 2006.
- [41] Alexei Baevski, Yuhao Zhou, Abdelrahman Mohamed, and Michael Auli. wav2vec 2.0: A framework for self-supervised learning of speech representations. *Advances in neural information processing systems*, 33:12449–12460, 2020.
- [42] André Araujo, Wade Norris, and Jack Sim. Computing receptive fields of convolutional neural networks. *Distill*, 4(11):e21, 2019.
- [43] Alexey Dosovitskiy. An image is worth 16x16 words: Transformers for image recognition at scale. *arXiv preprint arXiv:2010.11929*, 2020.
- [44] A Vaswani. Attention is all you need. *Advances in Neural Information Processing Systems*, 2017.